

Quantitative Photospheric Spectral Analysis of the Type IIP Supernova 2007od

C. Inserra^{1,2,3*}, E. Baron^{3,4,5}, M. Turatto⁶

¹*Dipartimento di Fisica ed Astronomia, Università' di Catania, Sezione Astrofisica, Via S.Sofia 78, 95123, Catania, Italy*

²*INAF Osservatorio Astrofisico di Catania, Via S.Sofia 78, 95123, Catania, Italy*

³*Homer L. Dodge Department of Physics and Astronomy, University of Oklahoma, Norman, OK 73019 USA*

⁴*Hamburger Sternwarte, Gojenbergsweg 112, 21029 Hamburg, Germany*

⁵*Computational Research Division, Lawrence Berkeley National Laboratory, MS 50F-1650, 1 Cyclotron Rd, Berkeley, CA 94720 USA*

⁶*INAF Osservatorio Astronomico di Trieste, Via Tiepolo 11, 34143, Trieste, Italy*

Received.....; accepted.....

ABSTRACT

We compare and analyze a time series of spectral observations obtained during the first 30 days of evolution of SN 2007od with the non-LTE code PHOENIX. Despite some spectroscopic particularities in the Balmer features, this supernova appears to be a normal Type II, and the fits proposed are generally in good agreement with the observations. As a starting point we have carried out an analysis with the parameterized synthetic spectrum code SYNOW to confirm line identifications and to highlight differences between the results of the two codes. The analysis computed using PHOENIX suggests the presence of a high velocity feature in H_β and an H_α profile reproduced with a density profile steeper than that of the other elements. We also show a detailed analysis of the ions velocities of the 6 synthetic spectra. The distance is estimated for each epoch with the Spectral-fitting Expanding Atmosphere Method (SEAM). Consistent results are found using all the spectra which give the explosion date of JD 2454403 (29 October, 2007) and a distance modulus $\mu = 32.2 \pm 0.3$.

Key words: supernovae: general - supernovae: individual: SN 2007od - line: identification - galaxies: distances and redshifts

1 INTRODUCTION

SN 2007od was discovered on 2007 November 2.85 UT in the nearby galaxy UGC 12846 (Mikuz & Maticic 2007). Blondin & Calkins (2007) classified it as a normal SN IIP about two weeks after explosion, and reported some similarity with the spectrum of the type II SN 1999em, 10 days after explosion. SN 2007od exploded in the Magellanic Spiral (Sm:) galaxy UGC 12846, which has a heliocentric recession velocity of 1734 ± 3 km s⁻¹, a distance modulus of 32.05 ± 0.15 and an adopted reddening of $E_{\text{tot}}(B-V) = 0.038$ (Inserra et al. 2011). Extensive studies of the photospheric and nebular periods have been presented in Andrews et al. (2010) and Inserra et al. (2011).

SN 2007od showed a peak and plateau magnitude, $M_V = -18.0$ and $M_V = -17.7$ respectively (Inserra et al. 2011), brighter than common SNe IIP (Patat et al. 1994; Richardson et al. 2002), but the luminosity on the tail is comparable with that of the faint SN 2005cs (Pastorello et

al. 2009). The luminosity on the tail was affected by the early formation of dust ($\lesssim 220$ d after explosion, Andrews et al. 2010). Based on mid infrared (MIR) observations in the nebular phase, the amount of dust has been determined to be up to $4.2 \times 10^{-4} M_\odot$ (Andrews et al. 2010) and the ejected mass $^{56}\text{Ni} \sim 2 \times 10^{-2} M_\odot$ (Inserra et al. 2011).

This object also shows interaction with a circumstellar medium (CSM). There is some evidence, in the form of high velocity features, for weak interaction soon after the outburst and solid observational evidence for interaction in the nebular phase (Inserra et al. 2011). However, due to the good temporal coverage, the position inside the host galaxy, and the low observed reddening, this supernova is a good candidate for analysis by the generalized stellar atmosphere code PHOENIX in order to learn more about its physical structure. In § 2 we present the codes and the strategy applied for modeling. In § 3 we show the synthetic spectra and the comparison with observed spectra, while in § 4 we provide an analysis of the principal characteristics of the synthetic spectra. A conclusion follows in § 5.

* E-mail: cosimo.inserra@oact.inaf.it(CI)

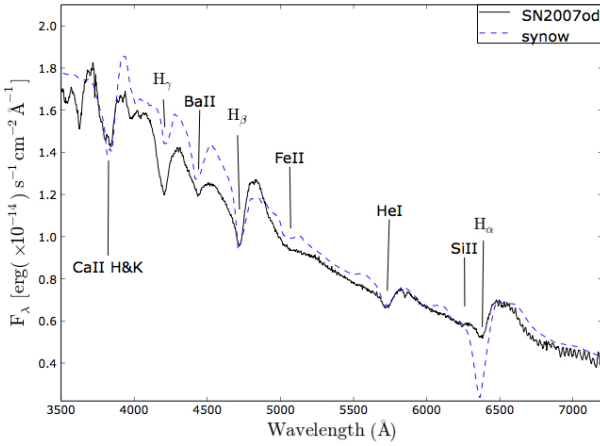


Figure 1. Comparison between the optical spectrum of SN 2007od at 5 days post explosion (JD 2454404) and the SYNOW synthetic spectrum (for composition of synthetic spectra see text).

2 METHOD

The preliminary line identification in the spectra of SN 2007od, confirming those obtained by Inserra et al. (2011), has been performed using the fast, parameterized supernova synthetic spectra code SYNOW. The code is discussed in detail by Fisher (2000) and recent applications include Branch et al. (2002), Moskvitin et al. (2010), and Roy et al. (2011). SYNOW assumes the Schuster-Schwarzschild approximation and the source function is assumed to be given by resonant scattering, treated in the Sobolev approximation. It correctly accounts for the effects of multiple scattering.

For a subsequent, more detailed analysis, we have used the generalized stellar atmospheres code PHOENIX (Hauschildt & Baron 2004, 1999). The code includes a large number of NLTE and LTE background spectral lines and solves the radiative transfer equation with a full characteristics piecewise parabolic method (Hauschildt 1992) without simple approximations such as the Sobolev approximation (Mihalas 1970). The process that solves the radiative transfer and the rate equations with the condition of radiative equilibrium, is repeated until the radiation field and the matter converge to radiative equilibrium in the Lagrangian frame. These calculations assume a compositionally homogeneous atmosphere with a power law density and steady state conditions in the atmosphere.

3 SPECTRA MODELS

We have modeled the first six observed photospheric spectra, covering a period from 5d to 27d since the adopted explosion date $JD = 2454404 \pm 5$ (~ 30 Oct. 2007, Inserra et al. 2011). The most interesting spectra are the first one of the series (5d), with a flat top H_α profile and two uncommon features at about 4400Å and 6250Å, and the last one (27d), which has the best signal to noise ratio among the plateau spectra. The detailed, comparative study of these epochs provides important information about the presence of ions and possible CSM interaction at early times.

Figure 1 shows the line identifications determined by the SYNOW analysis for the first spectrum, obtained using

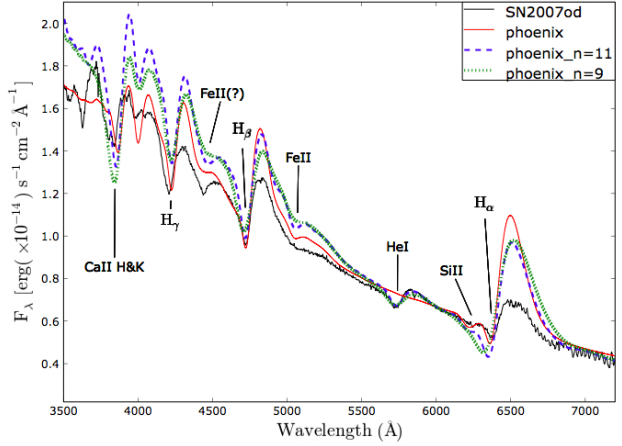


Figure 2. Comparison between the optical spectrum of SN 2007od at 5 days post explosion (JD 2454404) and PHOENIX full NLTE spectra. The model parameters are those of the first row of Tab. 1 but for the n index reported in the legend.

$T_{bb} \sim 12000$ K, $v_{phot} \sim 7800$ km s $^{-1}$, optical depth $\tau(\nu)$ parameterized as a power law of index $n = 9$, and $T_{exc} = 10000$ K assumed to be the same for all ions. The features visible in Fig. 1 are produced by only 6 chemical species. The P-Cygni profile of the Balmer lines are clearly visible, as well as He I $\lambda 5876$, and significant contributions due to Ca II, Fe II, Ba II, and Si II. The Balmer lines have been detached from the photosphere to better match the observed velocity. The uncommon lines mentioned above are identified as Ba II ($\lambda 4524$) and Si II ($\lambda 6355$). In our attempts we have considered also the possible presence of N II $\lambda 4623$, but the poor fit and the lack of N II $\lambda 5029$ and N II $\lambda 5679$ lines (stronger than the first one), lead us to the conclusion that there is no enhanced N in the spectra of SN 2007od (cfr. Inserra et al. 2011).

With the adopted reddening ($E(B-V) = 0.038$) and the ions suggested by the SYNOW analysis, we have computed a grid of detailed fully line-blanketed PHOENIX models. We have explored variations in multiple parameters for each epoch adjusting the total bolometric luminosity in the observer's frame (parameterized by a model temperature, T_{model}), the photospheric velocity (v_0), the metallicity (the solar abundances were those of Grevesse & Sauval 1998) and the density profile (described by a power law $\rho \propto r^{-n}$). Gamma-ray deposition was assumed to follow the density profile. We noticed an increase of the emission profiles, especially those of Balmer lines, with the increase of gamma ray deposition. However, in our final models the gamma-ray deposition was **not included**. We have estimated the best set of model parameters by performing a simultaneous χ^2 fit of the main observables. The relevant parameters for SN 2007od for the entire early evolution are reported in Tab. 1 while the fits are shown in Fig. 3.

In the first PHOENIX spectra we have treated in NLTE the following ions: H I, He I-II, Si I-II, Ca II, Fe I-II, Ba I-II. He I, Si I, Fe I and Ba I have been considered to reproduce the ionization levels of the corresponding atoms. The opacity for all other ions is treated in LTE with a constant thermalization parameter $\epsilon = 0.05$ (see Baron et al. 1996b, for further details). As shown in Fig. 2 there is no line that

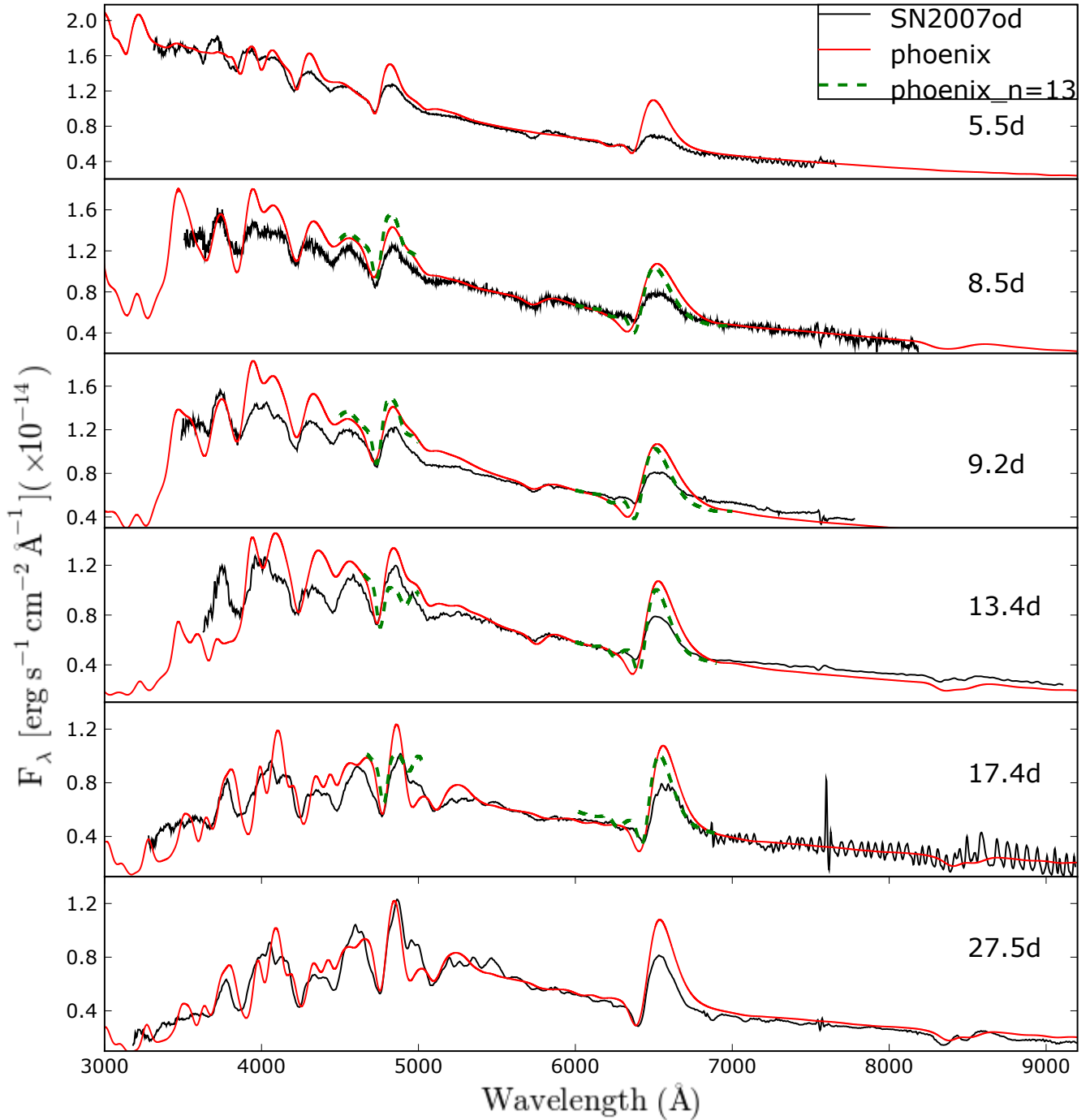


Figure 3. PHOENIX spectral evolution compared with observed spectrum. Model parameters for best fit spectra (red) are listed in Tab. 1. The dashed green lines in the spectra between day 8.5 and 17.4 in the H_β and H_α regions are the line profiles computed with a density index $n=13$.

corresponds to Ba II, even though the identification for the absorption at 4400\AA seemed plausible in the SYNOW analysis. The temperature is too high to produce a Ba II line, all the more so with the observed strength. The presence of Ba II was checked by calculating a set of single ion spectra, that is calculating the spectrum with all continuum opacities, and only lines from Ba II as well as via the inverse procedure of turning off the line opacity from Ba II. The same procedure

was performed for the He I ion, in order to study the feature that could arise around 4471\AA but no significant contribution can be seen in the synthetic spectra. The closest line to the 4440\AA feature is due to Fe II, though it is not as strong as in the observed spectrum. The evolution of the 4440\AA region (shown in Fig. 4) displays the inconsistency. The Fe II line explains the feature starting from day 9, though the velocity does not match the observed line position. It is likely

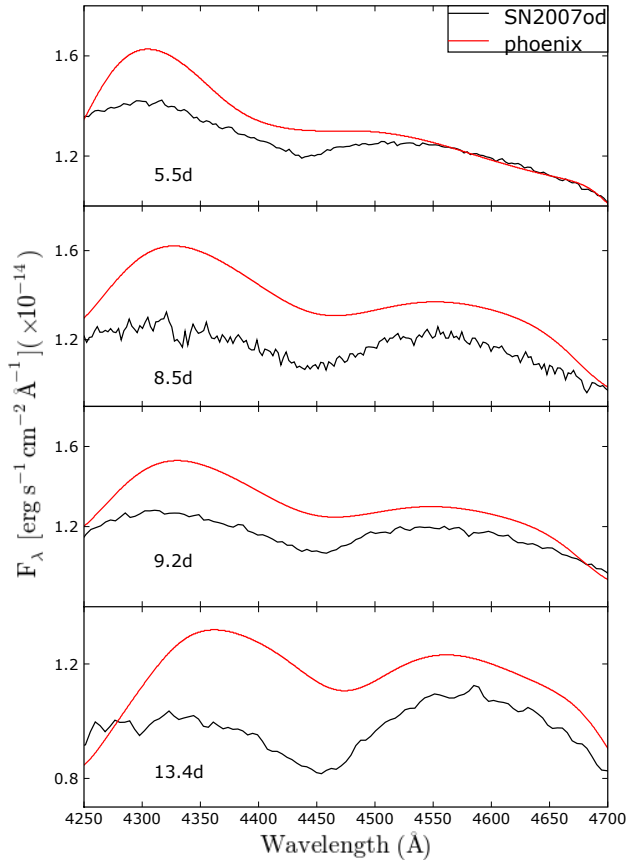
Table 1. Parameters of PHOENIX models of SN 2007od.

JD +2400000	Phase* (days)	T_{model}^\diamond (K)	v_0 (km s ⁻¹)	n^\dagger	r (10 ¹⁴ cm)	L (10 ⁴¹ erg s ⁻¹)
54409.5	5.5	8000	7600	13	3.6	3.8
54412.5	8.5	7400	7200	9	5.3	6.0
54413.2	9.2	7300	7050	9	5.6	6.3
54417.4	13.4	6800	6000	9	6.9	7.2
54421.4	17.4	6200	5400	9	8.1	6.9
54431.5	27.5	6000	5000	9	11.9	13.1

* with respect to the explosion epoch (JD 2454404) from (Inserra et al. 2011)

$^\diamond$ with a total E(B-V)=0.038 (Inserra et al. 2011)

† index of power law density function

**Figure 4.** A blowup of the 4440 Å region where the PHOENIX synthetic spectra are compared to observed ones.

that the observed profile of the 4440 Å feature is due to the combination of this line with high velocity feature (HV) of H_β , formed by an increased line opacity that our simplified model ($\rho \propto r^{-n}$) is not able to reproduce (the HV features are discussed in Inserra et al. 2011). Though Ba II identification provided by SYNOW is not completely ruled out by the NLTE analysis, however we consider it unlikely.

The presence of Si II at 6350 Å is confirmed by the PHOENIX analysis, despite the weakness of the synthetic feature. In Fig. 2 it is barely visible, but the same analysis

performed for Ba II confirms its identification. The presence of Si II in SNe IIP is not uncommon. The other absorption features are successfully reproduced, except for H_α (see § 4) and the absorption lines in the region of 3600 Å that are possibly related to Ti II, not included in the first NLTE spectra in order to minimize CPU time. As shown in Fig. 2 we tried different density indices to better match the entire profile. The best match for the overall spectrum is given by the model with $n=13$ (in all figures the best PHOENIX model is always plotted in red), even if the strengths, with respect to the normalized continuum, of H_γ and He I are better reproduced by the models with a density exponent lower than $n = 13$. The steeper density profile leads to greater emission than models with flatter density profiles.

Both the second (8.5d) and third (9.2d) spectra have been constructed using the same setup that was used to calculate the first spectrum, except that the density index was decreased from 13 to 9. A profile steeper than $n=9$, better reproduces the absorption profile of the Balmer lines, as seen in first epoch, but all the models show flux slightly higher blueward of 5500 Å and especially at about 4000 Å. Also the strength of H_γ is greater than observed in the model with $n > 9$. The flux on the blue side of Ca II H&K is lower than observed. We found that a steeper density profile enhances the discrepancy between the observed and synthetic H&K line profile.

In general, the line profiles suggest a density distribution more complex than a single power law. Our calculations suggest that perhaps a broken power law would better reproduce the observed spectra, with a shallower density profile at lower velocities and a steeper profile at higher velocities. The Ca II or He I ions are clearly better reproduced by a density index close to 9, while the metal elements (e.g. Fe and Si) which form close to the photosphere (and are relatively weak) are less sensitive to the assumed density profile. The Fe I-II and Si II are well reproduced with all density profiles, even if the steeper profile better reproduces the Si II profile than the flatter profile (see Fig. 2). While the more complex density profile could be intrinsic in the initial structure it is also possible that early interaction of the SN ejecta with a close in circumstellar region affect the line profiles. Indeed, the flat topped nature of the Balmer lines may indicate circumstellar interaction. A broken power law density distribution of the ejecta has been claimed also by Utrobin & Chugai (2011) in the case of SN 2000cb. To illustrate the case we have over-plotted in Fig. 3 the H_β and H_α regions obtained by $n=13$ models (green dashed line) for the spectra from 8.5d to 17.4d.

The spectra at 13.4 and 17.4 days show the increasing effects of a few metal lines such as Fe II $\lambda 5169$ and Sc II $\lambda 6300$ that indicate the lower temperature at the beginning of the plateau phase. Moreover, the presence of metal ions changes the flux at ~ 3800 Å in the spectra at 13d. From this epoch onward, the 4440 Å feature seems more clearly related to Fe II, strengthening our conclusion for the absence of Ba II.

The final spectrum we analyze was obtained on November 27, 2007 (27d) when the supernova is solidly on the plateau. At this epoch the metal lines are fully developed, as is the Na ID feature that has replaced the He I $\lambda 5876$ line. Thanks to the broad wavelength coverage, the good resolu-

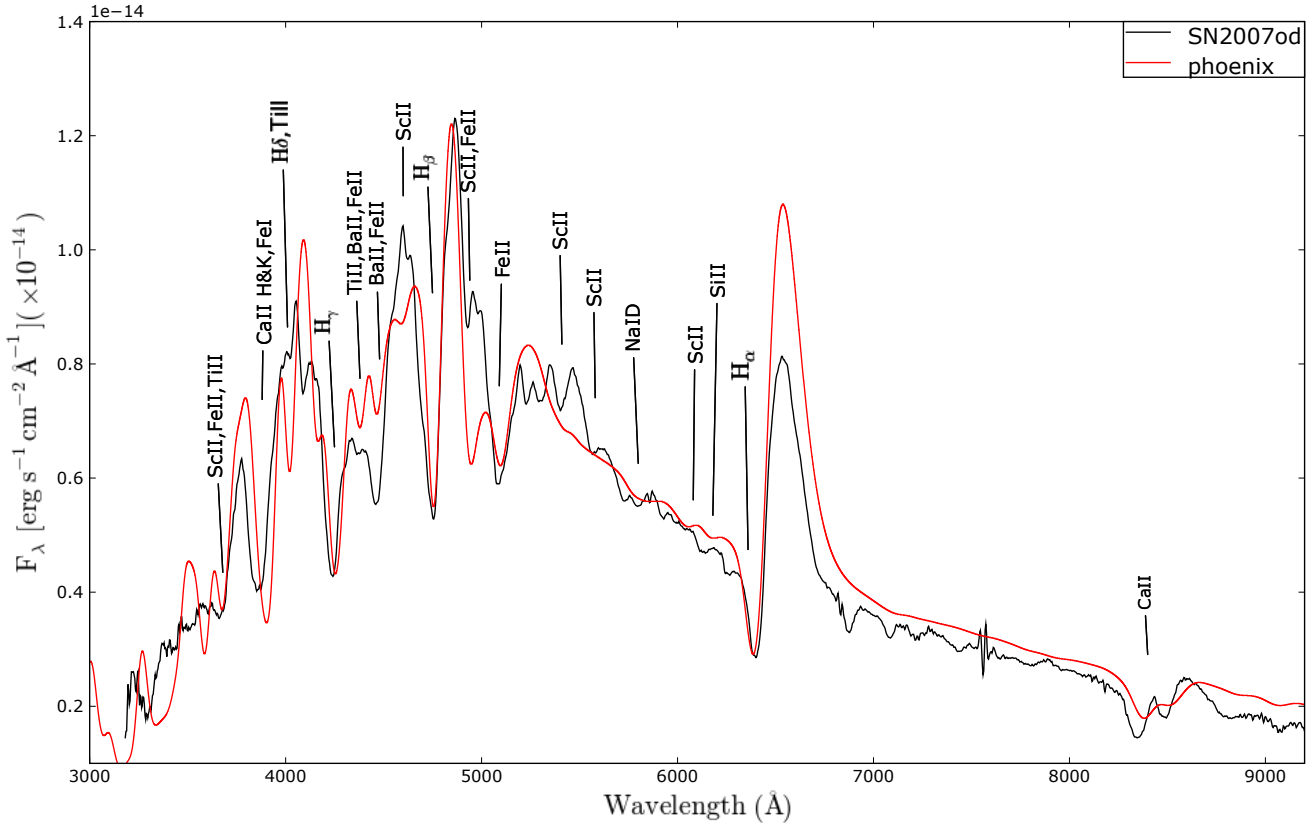


Figure 5. Comparison between the optical spectrum of SN 2007od at 27 days post explosion (JD 2454404) and the PHOENIX full NLTE spectrum (for model parameters see Tab. 1).

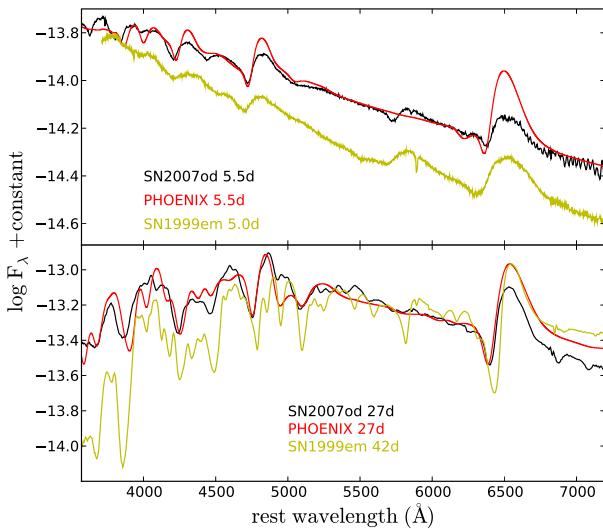


Figure 6. Comparison between observed spectra of SN 2007od, PHOENIX full NLTE spectra (for model parameters see Tab. 1) and SN 1999em spectra at the first (top) and last epoch (bottom) of our series.

tion (11Å), and the high signal to noise (S/N=60), this is the best available spectrum of SN 2007od.

Fig. 5 displays our best NLTE model. The species treated in NLTE are H I, Na I, Si I-II, Ca II, Sc I-II, Ti I-II, Fe I-II and Ba I-II. Here, more than at earlier epochs, the presence of the neutral species change the strength of some lines, especially in the blue ($< 4000\text{\AA}$) and around 5000\AA . The H lines, Na ID, Fe II $\lambda 5169$, Sc II $\lambda 5658$, and $\lambda 6245$ are well fitted. The Ca II lines also are well fitted. Other lines fit fairly well in terms of velocity width, but not necessarily in total flux. This is due to the fact that many lines are blended with others.

All models have solar abundances and metallicity. We studied the effects of reducing the model metallicity to that deduced for the SN 2007od environment $Z < 0.004$ (see Inserra et al. 2011), but the changes in the spectra were negligible at the 3σ level.

The comparative evolution of SN 2007od has been discussed in Sect. 3.3 of Inserra et al. (2011). The most interesting features noticed in the earliest phases were the 4400\AA absorption and the boxy profile of the Balmer lines. In Fig. 6 we compare the spectra of SN 2007od at two phases (day 5.5 and day 27) with those of SN 1999em, the most similar SN IIP as determined by GELATO analysis (Harutyunyan et al. 2008), and with the two corresponding best synthetic spectra. Indeed the overall similarity is remarkable. However there are also interesting differences, in addition to the two major ones mentioned above. At the first epoch the expansion velocity

is larger in SN 1999em ($\text{FWHM}(\text{H}_\alpha)_{99\text{em}} \sim 11000 \text{ km s}^{-1} > \text{FWHM}(\text{H}_\alpha)_{07\text{od}} \sim 9000 \text{ km s}^{-1}$) while at the second epoch SN 2007od is faster than SN 1999em ($\text{FWHM}(\text{H}_\alpha)_{07\text{od}} \sim 7000 \text{ km s}^{-1} > \text{FWHM}(\text{H}_\alpha)_{99\text{em}} \sim 5500 \text{ km s}^{-1}$). However, the epochs are offset so evolution could play a role. The slower velocity evolution of SN 2007od was already noticed by Inserra et al. (2011). The model is able to reproduce consistently the spectra of SN 2007od at both epochs. The **other** major difference is in the line contrast. Considering the ongoing early interaction, we can interpret the effect as due to toplighting (Branch et al. 2000) which smooths the line contrast. At the second epoch the difference between the line profiles of the two objects and the model is reduced.

4 ANALYSIS

The expansion velocities of H_α , H_β , $\text{He I } \lambda 5876$, and $\text{Fe II } \lambda 5169$ as derived from fitting the absorption minima of the PHOENIX spectra, are shown in Fig. 7 together with the measured values in the observed spectra. The filled symbols indicate the spectra shown in Fig. 3 (reported in Tab 1), while the open symbols refer to spectra calculated with different density indexes ($n = 9$ for the first epoch, $n = 13$ for the following epochs).

In Fig. 7 (top left panel) and Fig. 3 the absorption minima in the NLTE ($n=9$) spectra for H_α are too blue when compared with the observed spectra, particularly for the first three epochs. Instead the models with $n=13$ better reproduce the observed velocity. This could be due to several effects. The simple uniform power-law density profile, assumed here, may be not accurate enough to describe the ejecta. Also ionization effects, perhaps due to circumstellar interaction, may reduce the Balmer occupations over those that are predicted in the $n = 9$ models. Combined with the evidence of the flat-top emission, it is somewhat possible that circumstellar interaction effects are responsible for the observed shape of the Balmer lines and for the different density profiles. The effect disappears with time. Also for H_β , the PHOENIX and the observed velocity from 13.4d are comparable within the errors for both models. From day 8.5 and onward the $n = 9$ models better reproduce the H_β profile in velocity and strength. Neither He I nor Fe II show this behavior in the early epochs, indicating that the effect is most likely confined to the outermost layers of the ejecta. Except for the epochs reported above, all the line velocities are slightly smaller than observed. Though we have not included time-dependent rates in this calculation, this effect seems not so likely to explain the discrepancy between the velocity of the synthetic and observed H_α (Utrobin & Chugai 2005; Dessart & Hillier 2007; De, Baron, & Hauschildt 2009, 2010).

Clearly our simplistic models do not reproduce the HV feature of H_β and overestimate the emission strength of H_α , especially in the first spectrum. While interaction of the SN ejecta with circumstellar matter may be important, it is also possible that the density distribution we have adopted is too simplistic. The latter highlights the need for using the correct physical structure when modeling the SNe.

The sample of photospheric NLTE spectra collected for the SN 2007od **allow to apply the** Spectral-fitting Expanding Atmosphere Method (SEAM, Baron et al. 1993; Baron,

Hauschildt, & Branch 1994; Baron et al. 1995, 1996a) since in addition to a good overall shape of the spectra, the models predict consistent fluxes. We can derive a distance modulus by subtracting our calculated absolute magnitudes from the published photometry (Inserra et al. 2011), assuming a reddening of $E(B-V)_{\text{tot}} = 0.038$. Considering all the epochs, we obtain the distance modulus of the supernova, $\mu = 32.5 \pm 0.3$ where the errors include the standard deviation of our fits and the error due to the uncertainty in the interstellar reddening. Since SEAM is strongly dependent on the uncertainties of the explosion date, it seems reasonable to give lower weight to early spectra, since a longer time baseline minimizes the error due to the uncertainties in the explosion day. If we consider only the later observed spectra, from 13.4d to 27.5d, we find $\mu = 32.2 \pm 0.2$, in good agreement with the value reported in Inserra et al. (2011). Furthermore, model spectra for the last three epochs better fit the observations over the entire spectral range, and the derived distance modulus is comparable with the Mould et al. (2000) measurement within the uncertainties.

Indeed, a good agreement with the Inserra et al. (2011) distance ($\mu = 32.2 \pm 0.3$) is obtained by using all spectra and by taking the explosion date to be JD 2454403 (29 October, 2007). Hence we conclude that the explosion date is October 29 ± 1.5 days. The explosion date should always be determined by a χ^2 minimization in a SEAM analysis.

5 CONCLUSIONS

We have shown that both direct synthetic spectral fits and detailed NLTE models do a good job in reproducing the observed optical spectra of SN 2007od. We have also pointed out that detailed NLTE spectral modeling of early spectra does not support the line identification (Ba II, Fe II or He I) of the 4440Å as suggested by the SYNOW model or as identified in previous SNe IIP. Rather we interpret the line as a combination of Fe II and with an additional contribution from a possible HV feature of H_β . The origin of the line could be due to increased opacity at high velocities due to variation in the level populations not accounted in the simple density profile of PHOENIX or due to possible interaction in the outermost layers. This result suggests extreme caution with line identifications in hot, differentially expanding flows. At the same time it shows that PHOENIX calculations give reliable results and lend support to the reliability of the modeling. Our spectral analysis shows that during the plateau Sc II lines can arise even with standard solar abundances. Also Si II lines are reliably identified in the spectra of our relatively normal SN IIP at early times. Another important issue is related to the difference between the density profile ($\rho \propto r^{-13}$) needed to reproduce H_α from 8.5d to 17.4d and the density law required to reproduce the other elements ($\rho \propto r^{-9}$). The evidence for a broken power law density profile shown by SN 2007od could be a general property of type II SNe or maybe a consequence of a perturbed ejecta, especially in the outermost layers. We have also **discussed** the velocity and strength evolution of the principal lines. We have also applied the Spectral-fitting Expanding Atmosphere Method (SEAM) to SN 2007od obtaining good agreement with the distance modulus provided in Inserra

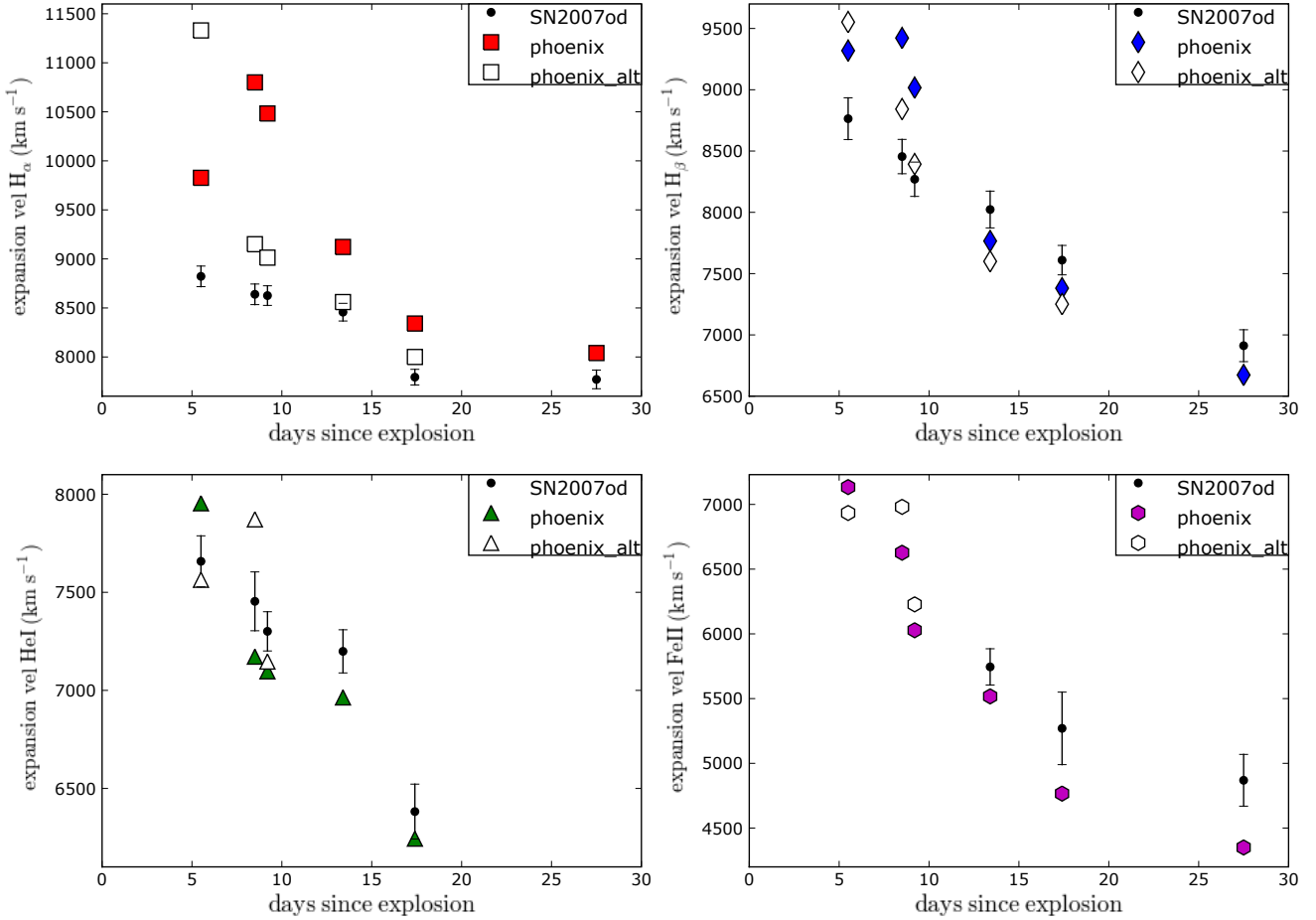


Figure 7. Expansion velocities of H α , H β , He I, and Fe II measured from synthetic PHOENIX NLTE spectra compared with those measured from the observed spectra (black dots with errorbars) by Inserra et al. (2011). Filled symbols refer to the spectra shown in Fig. 3, while open symbols to spectra calculated with different density indexes ($n = 9$ for the first epoch, $n = 13$ for the following).

et al. (2011) which allows to better constrain the explosion date (29 October, 2007).

ACKNOWLEDGMENTS

This work was supported in part NSF grant AST-0707704, and US DOE Grant DE-FG02-07ER41517 and NASA program number HST-GO-12298.05-A. Support for Program number HST-GO-12298.05-A was provided by NASA through a grant from the Space Telescope Science Institute, which is operated by the Association of Universities for Research in Astronomy, Incorporated, under NASA contract NAS5-26555. C.I. thanks David Branch for the useful discussions. M.T. is partially supported by the PRIN-INAF 2009 “Supernovae Variety and Nucleosynthesis Yields”. We thank the anonymous referee for the useful suggestions that improved our paper.

REFERENCES

- Andrews J. E., et al., 2010, ApJ, 715, 541
- Baron E., Hauschildt P. H., Branch D., Wagner R. M., Austin S. J., Filippenko A. V., Matheson T., 1993, ApJ, 416, L21
- Baron E., Hauschildt P. H., Branch D., 1994, ApJ, 426, 334
- Baron E., et al., 1995, ApJ, 441, 170
- Baron E., Hauschildt P. H., Branch D., Kirshner R. P., Filippenko A. V., 1996, MNRAS, 279, 799
- Baron E., Hauschildt P. H., Nugent P., Branch D., 1996, MNRAS, 283, 297
- Blondin S., Calkins M., 2007, CBET, 1119, 1
- Branch D., Jeffery D. J., Blaylock M., Hatano K., 2000, PASP, 112, 217
- Branch D., et al., 2002, ApJ, 566, 1005
- De S., Baron, E., & Hauschildt, P. H., 2009, MNRAS, 401, 2081.
- De S., Baron, E., & Hauschildt, P. H., 2010, MNRAS, 407, 658.
- Dessart L., & Hillier, D. J., 2007, MNRAS, 383, 57.
- Fisher A., 2000, PhD thesis, Univ. Oklahoma
- Grevesse N., Sauval A. J., 1998, SSRv, 85, 161
- Harutyunyan A. H., et al., 2008, A&A, 488, 383
- Hauschildt P. H., 1992, JQSRT, 47, 433
- Hauschildt P. H., Baron E., 1999, JCoAM, 109, 41

- Hauschildt P. H., Baron, E. 2004, Mitt. Math. Ges., 24, 1
 Inserra C., et al., 2011, MNRAS, 417, 261
 Mihalas D., 1970, Stellar Atmospheres. Series of Books in
 Astronomy and Astrophysics. Freeman, San Francisco
 Mikuz H., Maticic S., 2007, CBET, 1116, 1
 Moskvitin A. S., Sonbas E., Sokolov V. V., Fatkhullin T. A.,
 Castro-Tirado A. J., 2010, AstBu, 65, 132
 Mould J. R., et al., 2000, ApJ, 529, 786
 Pastorello A., et al., 2009, MNRAS, 394, 2266
 Patat F., Barbon R., Cappellaro E., Turatto M., 1994,
 A&A, 282, 731
 Richardson D., Branch D., Casebeer D., Millard J., Thomas
 R. C., Baron E., 2002, AJ, 123, 745
 Roy R., et al., 2011, MNRAS, 637
 Utrobin V., & Chugai, N., 2005, A&A, 441, 271
 Utrobin V. P., Chugai N. N., 2011, A&A, 532, A100